International Journal of Civil Engineering, Construction and Estate Management
Vol.7, No.1, pp.117-146, March 2010
Published by European Centre for Research Training and Development UK (www.eajournals.org)

THE EFFECTS OF PARTIAL SHEAR CONNECTION ON COMPOSITE STEEL-CONCRETE BEAMS SUBJECTED TO COMBINED FLEXURE IN YEMEN

Abdulrahman Ali[1,*], Yu Zhixiang[2]

[12]School of Civil Engineering, Southwest Jiaotong University, Chengdu, Sichuan, China.

* Correspondence: shams5995@my.swjtu.edu.cn

ABSTRACT: *Composite steel-concrete development has been broadly utilized the world over. Procedures for a definitive load examination and plan of composite steel-concrete beams are additionally established, and arrangements can be acquired without any difficulty. Nonetheless, beams under joined activities, for example, an edge or bent in plan beams exposed to torsion and flexure can be hard to find out their strengths and conduct because of their mind-boggling stress state. These impacts of consolidated activities are not right now tended to in the American Standard ACI 2327.1 (Standards America, 2007) or any their universal codes.Along these lines, this paper will exhibit a full-scale test arrangement to examine the conduct of straight and curved in plan composite steel-concrete beams exposed to torsion and flexure with the impact of partial shear connection. Push-out and material tests were completed to decide the material properties of every segment of the composite steel-concrete beams.Another advancement of a 3-D finite element model display utilizing ABAQUS equipped for simulating composite steel-concrete beams exposed to combined flexure and torsion with the impact of partial shear connection. From the comparisons, the models were approved with the experimental outcomes and demonstrated great assention as far as load-deflection reaction and ultimate strengths. Parametric research was then led to examine the conduct of the beams under the impacts of various beam span lengths and dimensions of shear connection by broadening the finite element model. From the examination, composite steel-concrete beams have demonstrated an expansion in the torsional and flexural limits with the increment in span length, while the partial shear connection has no critical impact on its strengths. Moreover, the rate of increment in the torsional strength additionally increments with span length. Disentangled structure models have been proposed to speak to the flexure-torsion interaction relationship for both straight and curved in plan composite steel-concrete beams.*

KEYWORDS: Push out, Composite steel-concrete, torsion, flexure strengths, failure mode, ABAQUS

INTRODUCTION

At present, composite steel structures are used in civil engineering projects around the world such as applications including construction, bridges, tunnels, foundations and special structures (Bridges et al., 2006). Composite steel-concrete systems combine the advantages of a ductile steel frame with stiffness concrete slabs and then carry the loads. Also, provided that the steel frame supports construction loads,

Print ISSN: ISSN 2055-6578(Print)
Online ISSN: ISSN 2055-6586(online)

composite construction can reduce the period required for construction. Composite construction has been commonly used in modern buildings and highways because of its advantages over traditional reinforced concrete structures. However, due to some complexities in modern building designs, some supporting beams such as the edge or curved in the plan member are subject to combined loading. One of these combinations is the application of combined flexure and torsion. Combined loading effects are not currently processed in US standards or any other international codes. Therefore, this paper presented a study to investigate the behavior of composite steel-concrete beams exposed to combined flexure and torsion.

In this part, I present a summary of the research conducted in this paper, as well as their contributions and significance in the field of composite steel construction. The shortcomings were identified by an extensive background reading of the papers, which also highlighted the need for future research in composite steel-concrete construction, especially when using a partial shear connection (PSC). This paper seeks to verify the identified shortcomings, particularly about composite steel-concrete beams subjected to combined flexure and torsion. This field is further explained in the following parts as part of this scientific paper.

Experimental Program

This part presents the first experimental stage of a broader study of the behavior of composite steel-concrete beams exposed to combined flexure and torsion, in particular, the initial development of the rational design method for curved members of the plan.
All test specimens were tested for failure under different combinations of flexural and torsional loading. This chapter describes the design and construction of test specimens, test preparation, and instrumentation used to measure strength responses, test observations, and results.

DETAILS OF TEST SPECIMEN

Beam test specimens

Six beams of composite steel-concrete beams supported CBF-1, 2, 3, and CBP-1, 2 and 3 were tested under combined flexure and torsion. While CBP-1, 2 and 3 were designed with 50% shear connection. The length of each test specimens was 4.6 m and was simply supported span over 4 meters. The steel beams adopted were total beam sections in the cross-section of 200UB29.8. The thickness of the concrete slab is 120 mm, and the width is 500 mm. The steel beam was connected to the concrete slab by means of a 19 mm nominal diameter headed shear studs. Detailed geometric shapes of all composite steel-concrete test specimens in Figs.1 to Figs.6 show their cross-sectional views, plan and elevation.

Print ISSN: ISSN 2055-6578(Print)
Online ISSN: ISSN 2055-6586(online)

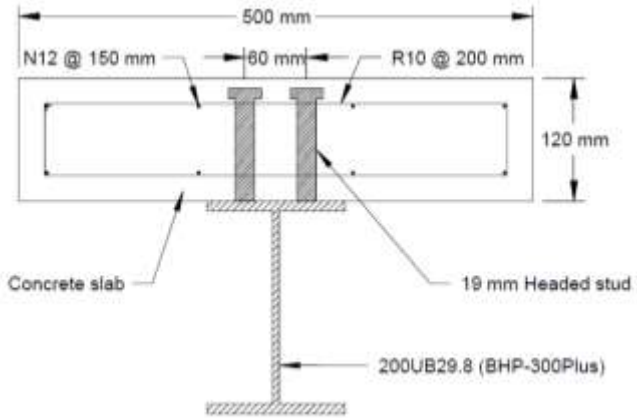

Figure.1 Cross-sectional views for CBF-1, CBF-2 and CBF-3

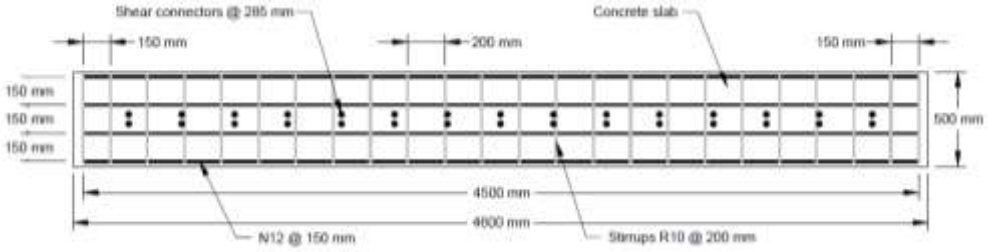

Figure.2 Plan view for CBF-1, CBF-2 and CBF-3

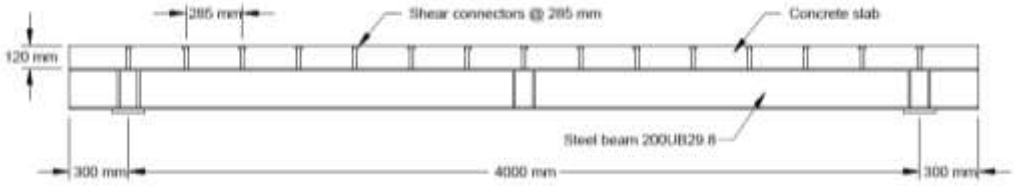

Print ISSN: ISSN 2055-6578(Print)
Online ISSN: ISSN 2055-6586(online)

Figure.3 Elevation view for CBF-1, CBF-2 and CBF-3

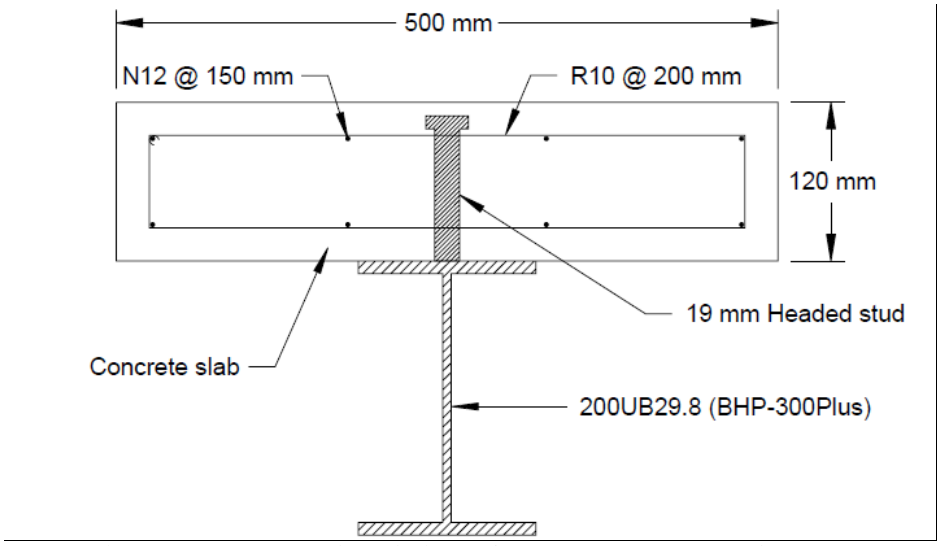

Figure.4 Cross-sectional views for CBP-1, CBP-2 and CBP-3

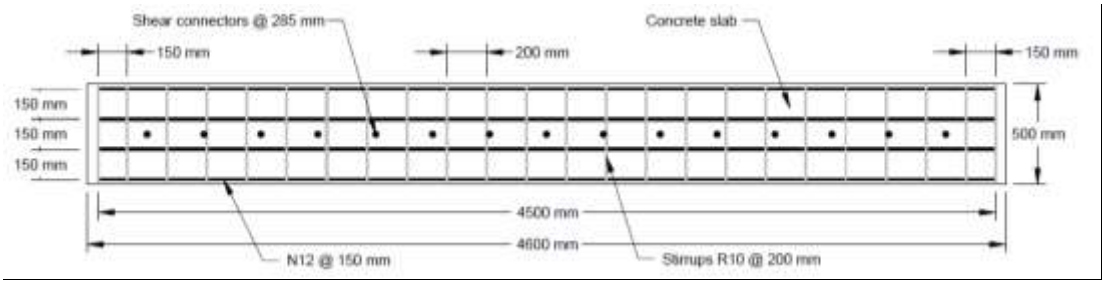

Figure.5 Plan view for CBP-1, CBP-2 and CBP-3

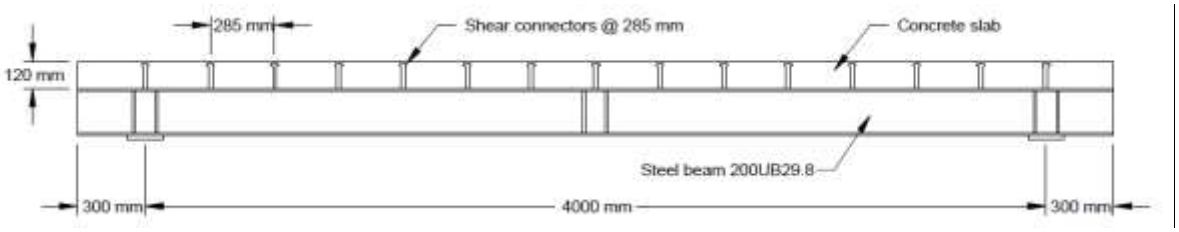

Figure.6 Elevation view for CBP-1, CBP-2 and CBP-3

The details of materials, engineering, and design of all composite steel-concrete beams are summarized in Table.1.

Print ISSN: ISSN 2055-6578(Print)
Online ISSN: ISSN 2055-6586(online)

Table.1 Straight beam specimen details

Specimen	Beam	A degree of shear connection (%)	Stud section(19 mm studs)	Total number of studs	Stud spacing (mm)	Load eccentricity from the centerline (mm)
CBF-1	Composite	100	2	30	285	0
CBF-2	Composite	100	2	30	285	100
CBF-3	Composite	100	2	30	285	175
CBP-1	Composite	50	1	15	285	0
CBP-2	Composite	50	1	15	285	100
CBP-3	Composite	50	1	15	285	175
Number of specimens			12			
Concrete slab size			4600 x 500 x 120 mm			
Concrete strength			32 N/mm²			
Concrete cover			25 mm			
Steel beam			200 UB 29.8 (BHP-300PLUS)			
Longitudinal reinforcement			N12 – Grade 500 N/mm²			
Transverse reinforcement			R10 - Grade 500 N/mm²			
Shear Studs			19 mm headed studs			

Push-out test specimens

Push-out tests were conducted to determine the slip-load characteristics and the ultimate shear capacity of the shear head studs used in experimental tests for the composite steel-concrete beam. Four push-out tests were conducted in this experimental. While the other two (PT-P1 and PT-P2) were implemented for composite steel-concrete beams of PSC as shown in Figure.7.

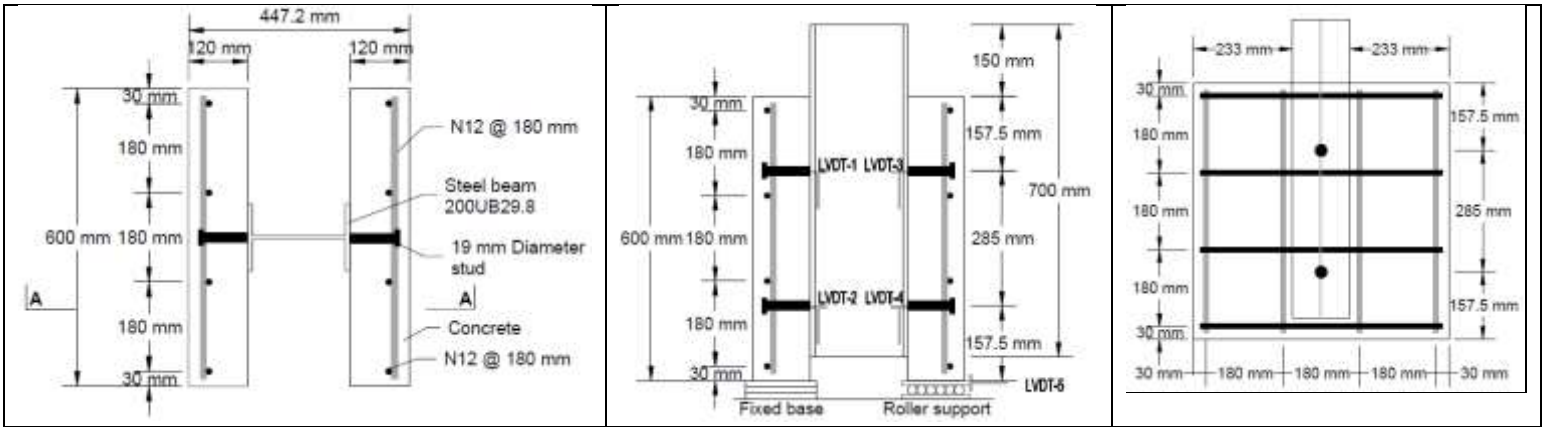

(a) Plan View (b) Cross-Sectional view A-A (c) Elevation View

Figure.7 Push-out test specimens for PT-P1 and PT-P2

Print ISSN: ISSN 2055-6578(Print)
Online ISSN: ISSN 2055-6586(online)

All were designed according to Eurocode 4 (British Standards Institution, 1992). The details of the push-out test specimens are summarized in Table.2.

Table.2 Push-out specimen details

Specimen	Stud section (19 mm studs)	Total number of studs	Stud spacing (mm)	Comment
PT-P1	1	4	285	PSC
PT-P2	1	4	285	PSC
Number of specimens			4	
Concrete slab size			600 x 600 x 120 mm	
Concrete strength			32 N/mm²	
Concrete cover			25 mm	
Steel beam			200 UB 29.8 (BHP-300PLUS)	
Reinforcement			N12 – Grade 500 N/mm²	
Shear Studs			19 mm headed studs	

TEST SPECIMEN FABRICATION

Beam test specimens

All beam test specimens were collected and assembled at the IBB University Structures Laboratory. The steel beams are supplied with the installed stiffeners web at the end of the supports and the middle of the steel beams. Plywood and shuttering molds are constructed to provide stability during the pouring of the concrete. The concrete beams were designed from the corners of the angled and bent steel, so that horizontal and diagonal surfaces were formed when welded at regular intervals on both sides of the steel beams.

Concrete slab soffit forms were constructed using plywood pieces to size and placed on steel supports. Screws and right angle were used to connect plywood forms together. Three beams were then aligned next to each other to provide better stability.Qualified stud fabricators have been employed to install shear studs on the top flange of the steel beam. The silicone sealant was applied to any gaps in the formwork before the formwork was removed and a coating of hydraulic oil was applied to the molds as a release agent when the molds were removed.

Reinforcing bars are prefabricated with steel cages using steel wire ties before placing them in formwork as shown in Fig.8. Reinforcing bar chairs were attached to a 25 mm height on the lower side of the crossbars in steel cages. Twisted 12 mm U-shaped bars are fabricated in the form of lifting lugs.

Print ISSN: ISSN 2055-6578(Print)
Online ISSN: ISSN 2055-6586(online)

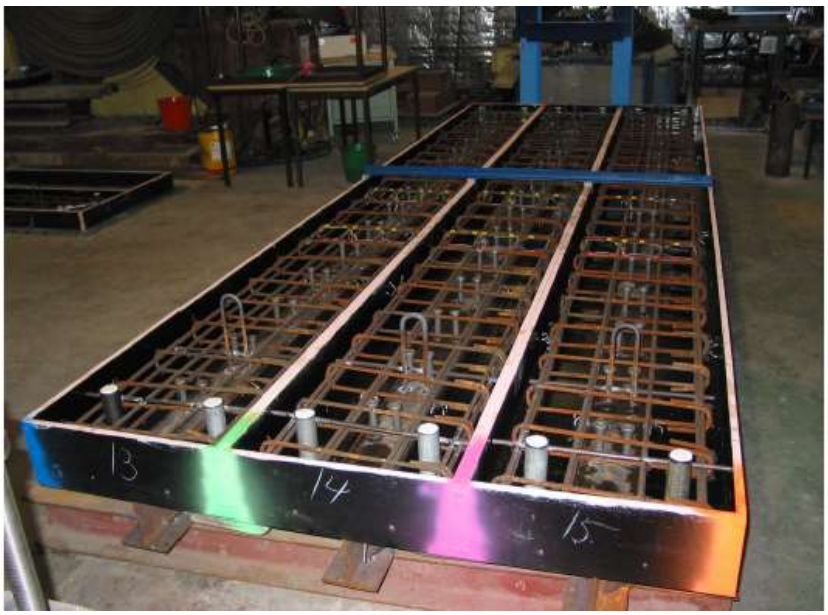

Figure.8 Beam test specimens ready for concrete casting

Each lifting handle was welded on the transverse reinforcing bar about 300 mm from the end of the formwork.

Standard cylinder molds were prepared for compressive and indirect tensile tests as shown in Fig.9. Concrete casting is made on materials, beams and push-out specimens. Concrete is placed in the molds using shovels and wheelbarrows.

The concrete was then compacted using the pneumatic vibrator. The exposed concrete surfaces were then finished with covering with polythene sheets and treated under wet conditions for 7 days. The models were then stripped after 14 days from the concrete pour.

Figure.9 Concrete cylinders

Print ISSN: ISSN 2055-6578(Print)
Online ISSN: ISSN 2055-6586(online)

Push-out test specimens

The push-out specimens are also prefabricated. The universal 200UB29.8 steel beam was cut from 200L29.8 of flame in T-sections while the concrete slabs were cast horizontally as shown in Fig.10. This procedure was in line with the guidelines provided by Code Eurocode 4 (British Standards Institution, 1992).

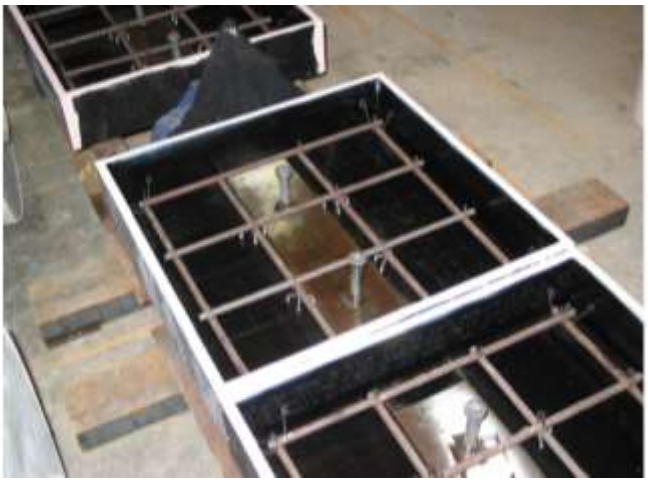

Figure.10 Push-out test specimens ready for concrete casting

Oehlers (1990) stated that if the concrete slab was cast vertically, there would be a significant risk of poor compaction at the base of the shear connectors. This weak compaction resulted in the air voids appearing in the concrete slab which subsequently reduced the shear capacity of the shear connectors. After 28 days of the time the concrete was poured, the two T-sections were welded together as shown in Figure.11.

Figure.11 Push-out test specimens welded together

Print ISSN: ISSN 2055-6578(Print)
Online ISSN: ISSN 2055-6586(online)

MATERIAL TESTS

Concrete

Concrete tests consist of standard cylinder compression and indirect tensile division tests. Tests were carried out at 7, 14, 21 and 28 and test days for test specimens and push-out. The AVERY 1800 KN compression testing machine was used to apply compressive strength at a load rate of 900 KN / min on concrete cylinders.

Structural steel

Universal steel beams of the 200UB29.8 cross section were used with a nominal yield strength of 300 N/ mm² in the experimental. However, standard tensile steel coupling tests were performed to determine the stress of flanges and steel flanges of steel beams used. Tensile tests have been performed and implemented according to AS1391 (Standards Australia, 1991) under the INSTRON 500 kW test instrument.

Four steel beam coupons were cut from a flange and four from the Internet with a nominal thickness of 9.6 and 6.4 mm respectively. The dimensions of the prefabricated steel coupons are shown in Fig. 12.

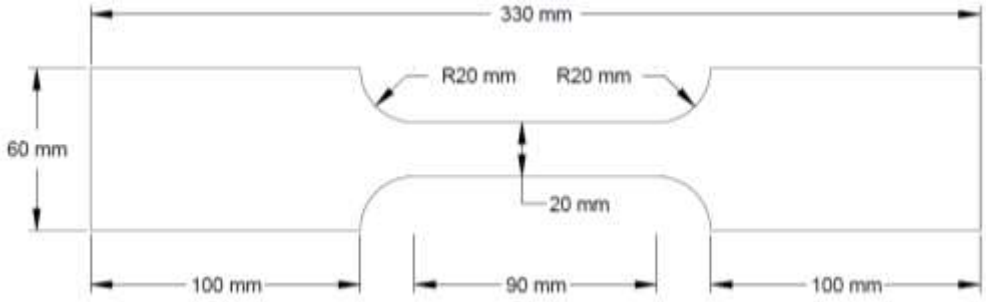

Figure.12 Steel coupons cut-out

During the tests, a 50mm gauge was used to measure the elongation and also to control the strain rate. Steel coupons were measured to determine their actual dimensions of width and thickness.

Steel reinforcing bar

N12 reinforcement bars were used with a nominal diameter of 12 mm as a longitudinal reinforcement in the concrete slabs, while the R10 stirrup reinforcement bars were used as torsion forces in concrete slabs with a nominal diameter of 10 mm. The longitudinal reinforcement bars were 500 Grade (fsy = 500 N / mm²) respectively and were standard bars with longitudinal ribs. The reinforcing bars were grade 400 (fsy = 400 N / mm²).

Five 400 mm length longitudinal reinforcing bars and five 400 mm stirrup reinforcement bars were cut for tensile tests to determine their stress according to AS1391 (Standards Australia, 1991).

Print ISSN: ISSN 2055-6578(Print)
Online ISSN: ISSN 2055-6586(online)

Shear Studs

Shear studs were tested in composite steel-concrete beam tests for vertical axial force due to the uplifting of concrete slabs from steel beams when torque was injected into composite steel-concrete sections. Therefore, it is logical to determine the tensile strength in the shearing studs. The tensile tests based on AS1391 (Standards Australia, 1991) were based. Shear studs are fabricated to the desired dimension as shown in Fig.13 for tensile tests.

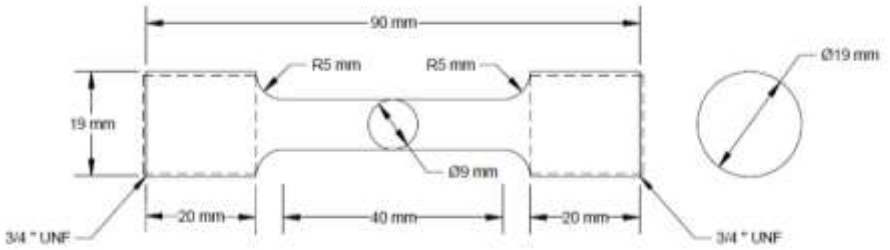

Figure.13 Shear stud cut-out

Five gear buttons were tested to provide tensile strength for the shear studs used in the composite steel-concrete beam tests. Their dimension and test results are summarized in Table.3.

Table.3 Headed shear stud tensile test results

Stud specimen	Diameter (mm)			Avg. diameter (mm)	Area (mm^2)	Max. load (kN)	0.2 % Proof stress (N/mm^2)	Tensile strength (N/mm^2)
1	8.85	8.85	8.84	8.85	61.5	28	422	455
2	8.75	8.76	8.75	8.75	60.1	36	434	599
3	8.94	8.94	8.90	8.93	62.6	35	414	559
4	8.44	8.46	8.44	8.45	56.1	31	420	553
5	8.72	8.72	8.72	8.72	59.7	32	413	536
						Avg.	421	540

Push-out test results

For the push-out PT-F1 test, the total load capacity of the shear studs reached a peak of 848 KN at a 2.5 mm front slip average. Therefore, the maximum load limit for each shear stud was determined at 106 KN. The load capacity remained similar until the vertical slip reached approximately 5.3 mm when the failure occurred. Early failure was observed and was found to be caused by the weakness of the weld that was performed on one of the shear studs. For Push-out test 2 (PT-F2), the maximum load capacity of the shear studs reached 870 KN at a 3 mm average interface slip. Therefore, the

Print ISSN: ISSN 2055-6578(Print)
Online ISSN: ISSN 2055-6586(online)

maximum load limit for each shear stud was determined at 109 KN. The load applied until the vertical slip remained approximately 10 mm when stud shank fracture failure occurred.

For push-out test 3 and 4 (PT-P1 and PT-P2), which represent the PSC shear stud arrangement, the peak load capacity was 422 and 454 KN, respectively. Therefore, the maximum loads for each shear stud 106 and 113 KN for PT-P1 and PT-P2, respectively.

The horizontal displacement of the roller support was drawn for the push-out tests as shown in Fig.14.

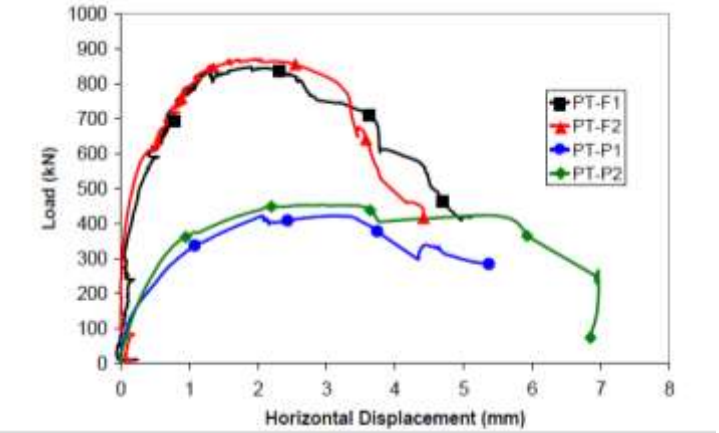

Figure.14 Load-horizontal displacements for push-out tests

Not all test samples that were push-out were excessive horizontal displacement during the tests, indicating the success of the push-out tests. The load limit applied to all push-out tests was reached before the horizontal displacement was 5 mm. Table.4 summarizes the results of the four push-out test. The maximum load average was calculated by dividing the maximum load applied with the number of shear studs in each test sample.

Table.4 Push-out test results

Push-out test specimen	Max. load (KN)	Max. load per stud (KN)	Avg. slip at max. load (mm)	Avg. slip at fracture (mm)
PT-F1	848.1	106	2.5	5.3
PT-F2	870.6	109	3	5.6
Avg.		108	2.8	5.5
PT-P1	422.4	106	6.6	8.7
PT-P2	453.7	113	5.6	12.0
Avg.		110	6.1	10.4

The sliding average was determined by averaging the values recorded from LVDT. From Table.4, we can conclude that there was no significant difference in shear capacity ability in shear studs for PSC. However, the PSC push-out test specimens provided a significant ductility, where the interface in shrinkage was higher in PSC push-out test specimens.

The phenomenon in which the ductility of the partial shear connection specimens is much lower than those containing full shear connection has been well detected and reported by Loh et al. (2004a & b).

Print ISSN: ISSN 2055-6578(Print)
Online ISSN: ISSN 2055-6586(online)

The results of the four push-out tests reinforced this phenomenon because the average 10.4 mm slip capability for PT-P1 and PT-P2 was higher than the PT-F1 and PT-F2 capacity of 5.5 mm. PT-P1 and PT-P2 were tested specimens push-out designed on the composite steel-concrete beams with PSC. As mentioned above, composite steel-concrete beams with higher torque will fail at an early stage of testing when CBF-3 and CBP-3 were compared with CBF-2 and CBP-2. In terms of torsional twist, there were high torsional twists for composite steel-concrete beams with PSC. This can be explained by the cracking of excess concrete cracking for composite steel-concrete beams that have disturbed the measurement from the inclinometers measures on the concrete surface.
Table.5 summarizes all the maximum strengths such as the load-carrying, flexural and torsional moment capacities in the beam test specimens.

Table.5 Straight beam test results

Beam specimen	Ultimate applied a load (kNm)	Deflection at maximum load (mm)	Deflection at failure (mm)	Ultimate torque moment (kNm)	Twist at maximum load (mRad)	Twist at failure (mRad)	Ultimate flexural moment (kNm)	Failure Mode
CBF-1	312	98	184	0	-	-	220	Concrete crushing
CBF-2	315	68	128	17	7	41	214	Concrete torsional cracking
CBF-3	286	43	47	28	21	37	197	Concrete torsional cracking
CBP-1	273	97	191	0	-	-	188	Concrete crushing
CBP-2	283	98	196	16	9	21	194	Concrete torsional cracking
CBP-3	255	45	52	24	14	17	177	Concrete torsional cracking

Numerical model development

Now we escribes the development of a 3D element model (FEM) capable of simulating composite steel-concrete beams prone to combined flexure and torsion with PSC effect. The model was developed by using ABAQUS. The importance of the properties of nonlinear materials and longitudinal and torsional interfaces between the concrete slab and the steel bundle in the model was taken into consideration. The model also provided an additional ability to think about the torsional behavior of composite steel-concrete beams. The results of the model will be used to compare with the test results described above.

ABAQUS was used to perform numerical analysis for the design and behavior of composite steel-

Print ISSN: ISSN 2055-6578(Print)
Online ISSN: ISSN 2055-6586(online)

concrete beams exposed to combined flexure and torsion.

ABAQUS / Standard was used in this paper, as it represents an ideal solution technology for the static event where high-accurate stress management solutions are as critical as the trials.

Material Constitutive Relationships

The constituent laws of the material are used to determine the stress-strain characteristics properties of the materials used in ABAQUS. The accuracy of the analysis depends on the constituent laws used to determine the mechanical behavior of the components. The objective of this section is to develop a reliable understanding of mechanical behavior to develop models of composite steel-concrete of finite elements that can accurately predict their behavior and ultimate strength when subjected to combined flexure and torsion. The main components affecting the behavior of concrete composite steel beams are concrete slabs, steel beams, reinforcement bars, and shear connectors. These components must be carefully designed to obtain an accurate result from finite element analysis.

Concrete

One of the main components of composite steel-concrete beams is the concrete slab. Concrete properties can be obtained from concrete cylinder compression tests and split. However, only the average concrete compressive and tensile strength are determined by the two tests.
Therefore, to introduce the full stress-strain property of concrete in ABAQUS, a concrete property model is required.

Concrete property

For the property of the material, the stress curve and the concrete strain proposed by Carreira and Chu (2005) were recommended for plain concrete at ambient temperature. The concrete stress is supposed to be in longitudinal compression up to 0.4 of the maximum compressive strength. Beyond this point, for concrete in tension, it is assumed that the tensile stress varies linearly with an increase in tensile strain up to 0.1 of the compressive strength of the concrete. After cracked the concrete, the tensile stress was reduced linearly to zero. The strain value was taken at zero strain to be 10 times the strain at failure. This assumption allowed continuity of analysis although the lower concrete layer cracked in tension.

However, for modeling failure due to torsion, different material properties are needed for the material to be inserted into ABAQUS. The concrete slab was divided into four different layers as shown in Figure.15.

Print ISSN: ISSN 2055-6578(Print)
Online ISSN: ISSN 2055-6586(online)

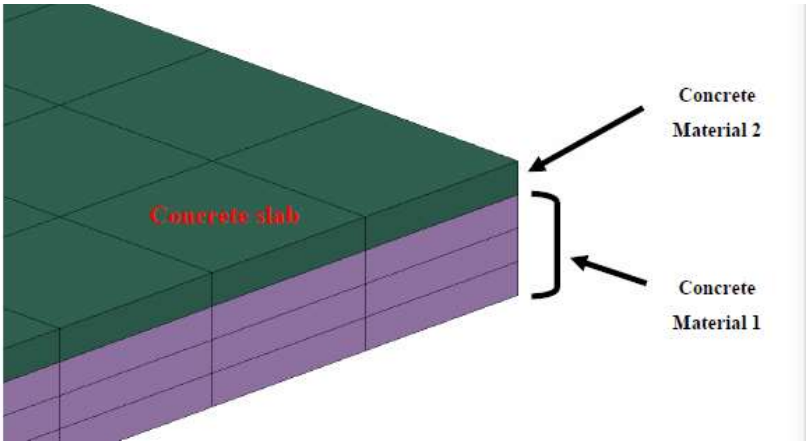

Figure.15 Concrete slab material properties allocation

Structural steel

The material properties of the steel beam and reinforcing steel are other basic components of the model. Curved stress-strain can be obtained for both steel beam and reinforce steel from hard tensile tests. The data were entered into two different material behaviors, elastic and plastic options for ABAQUS.

In the absence of material test results such as modeling for parametric study in the paper, the stress and strain curve of structural steel was proposed by Loh et al. (2014b). This curve was a simple elastic-plastic model with very stiffness. The behavior of the model is elastic at first, which develops after tenderness and stiffening as shown in Figure.16.

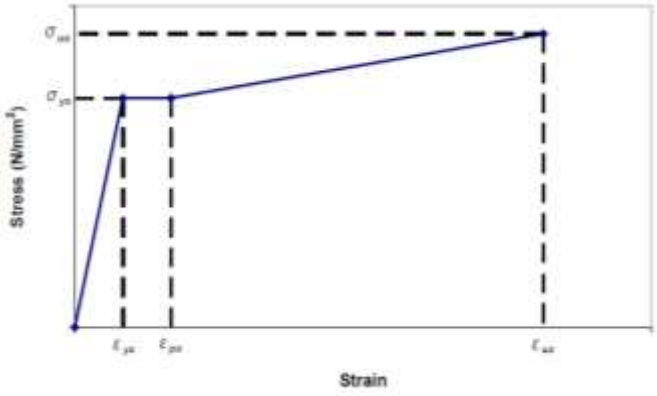

Figure.16 Stress-strain curves for structural steel

Luo et al. (2014b) found that simple linear lines were found to be accurate enough to represent the relationship between stress and strain. It was also assumed that the stress-strain curve was similar to structural steel in compression.

Print ISSN: ISSN 2055-6578(Print)
Online ISSN: ISSN 2055-6586(online)

Shear Studs

The most common type of shear connectors used in composite construction is vertical shearing studs. In each of the experimental, a 19 mm diameter inlay was used. The connectors provide the composite action between the steel beam and the concrete slab and prevent vertical separation between them in the front.

Contact Interactions and Boundary Conditions

Contact interactions and border conditions are important aspects of FEM. Since numerical simulation must take into account physical processes in surface and surface interactions and boundary conditions. Improper definition of boundary conditions may lead to non-physical effects in simulation, especially in this paper. There were more than two components considered in simulations such as concrete slabs, steel beams, reinforcing steel and shear studs.

Boundary conditions can be used to determine the values of basic solution variables such as displacement, rotation, deformation amplitude, fluid pressure, temperature, electrical potential, measured concentrations or acoustic pressure at the nodes. In this paper, boundary conditions are the ends that are simply supported by the steel beam and the twisted limits of the concrete slab. Karlsson and Sorensen (2016c) stated that most contact problems were designed using surface-based contact. The structures can be either 2-D or 3-D and can pass either with a small of finite sliding, for example, the surface of the interface between the concrete slab and the steel beam. Contact interactions can also be some types of kinetic constraints such as surface-based tie and surface-based surface constraints. Even boundary conditions are also a type of kinetic constraint in stress analysis because they define the support of the structure or give constant displacement in the nodal points. The contact interactions for FEM appear in Figure.17.

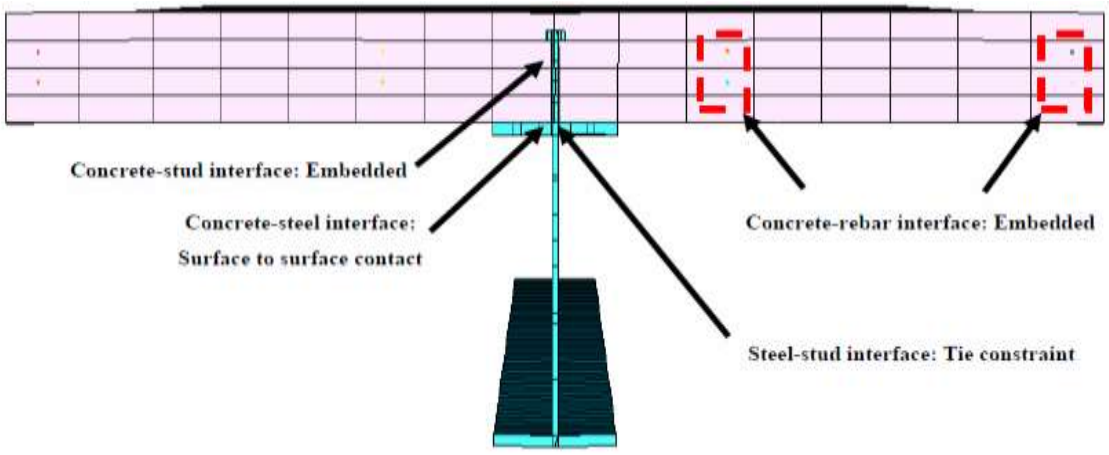

Figure.17 Contact interactions for FEM

Print ISSN: ISSN 2055-6578(Print)
Online ISSN: ISSN 2055-6586(online)

Steel beam and shear studs interface

Where the longitudinal interface slip is observed in the tests, thus FEM must be able to show in the analysis. There were contacts for the shear studs. One of the contacts parts was the upper part of the shear studs in the concrete slab, and the other was the connection of the shear studs to the top edge of the steel beam. A surface tie constraint was used to handle this interaction. They bind each decade of the contract to the bottom of the surface to obtain the same translated and rotational movements as well as all other degrees of active freedom as a point on the surface of the hard beams closest to it.

Simply supported and twisting restraint conditions

Since the composite steel-concrete beams were designed to be simply supported on both ends, it was necessary to restrain the concrete slab from torsion, so the boundary conditions for each support were determined. For the simply supported boundary condition, one end of the steel beam was described to restrict its U1, U2 and U3 translational displacements with the other party's support only with U2 and U3.

For the restriction condition, each of the terminal supports was bound by its U2 and U3 translational displacements to prevent the slab Concrete of torsion. The boundary conditions of the FEM are shown in Figure.18.

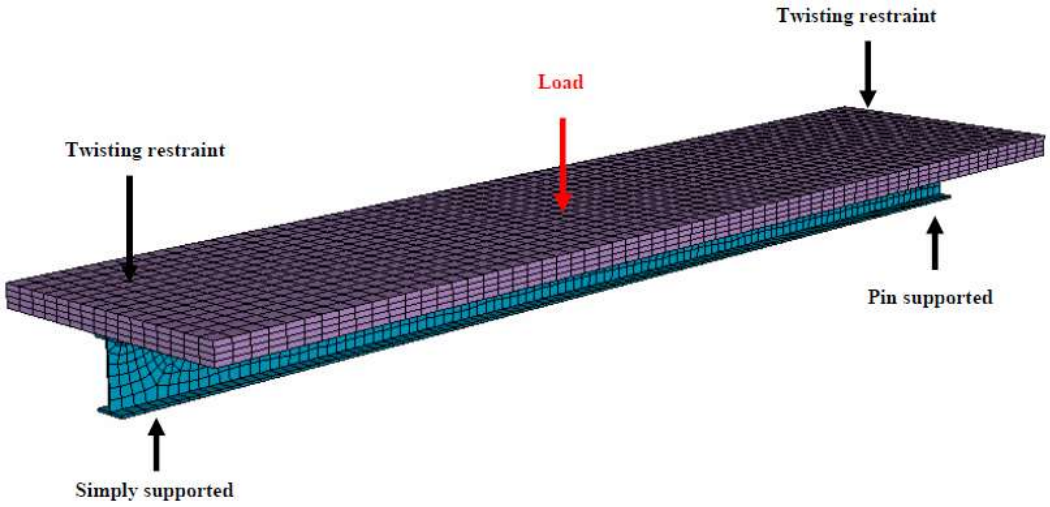

Figure.18 Boundary conditions for FEM

Concrete slab and shear studs interface

A similar restriction technique was used to simulate the contact interface between the concrete slab and the shear studs. Since one of the objectives of this paper is to examine the behavior of composite steel-concrete beams under the influence of a partial shear connection, FEM must be able to design or consider the longitudinal slip of the shear studs. The host element is the concrete slab while the upper surfaces of shear studs Built-in concrete slab.

Print ISSN: ISSN 2055-6578(Print)
Online ISSN: ISSN 2055-6586(online)

Concrete slab and reinforcing steel interface

The interface between concrete and reinforced steel was less important than another. It was assumed that there was no slippage between concrete and reinforcing steel during analysis. Therefore, the built-in constraint method was used in FEM. This embedded technique was used to identify the reinforcing bar elements that reside in the host element, which in this case was the concrete slab to be restricted. When the node of the eliminated compensatory enhancement element within the host element, the degrees of freedom in the node will be eliminated node will become "node built-in." The degrees of freedom of the steel knots were an integral part of the independent values of the degrees of freedom of the host element.

Concrete slab and steel beam interface

Because most contact problems were designed using surface contact, they were used to model the slipping contact interface between the concrete slab and the steel beam. To simulate the contact interface between these two different elements, the concrete was considered as the main surface and the steel as a surface of the slave. A small sliding formula was used to allow for large rotation, but the slave node would react with the same loading area of the main surface during analysis. To define the definition of the interface relationship, a "hard" connection relationship was used to reduce the penetration of the slave contract to the main surface and to prevent the transfer of tensile stress across the interface. For friction behavior in the interface, the contact property was used without friction.

Load Applications

Since this paper was looking at composite steel-concrete beams subjected to combined flexure and torsion, load applications played an important role in determining different levels of the parameter. Different sets of applied torque and bending loads have significant effects on the behavior of composite steel-concrete beams.

Applied load method

There are two ways to determine the distributed loads in ABAQUS: distributed loads based on elements and loads distributed on the surface. Element-based loading is used to determine the distributed loads on object objects and objects, while surface loading describes a load distributed on a surface. For this paper, the load was used on a surface basis because it provided a more realistic load than element-based loading. Therefore, the load applied to a pressure load on a specific surface is defined by the surface area of the steel plate loading in the experimental.

Modified Risk analysis method

The modified risk method was used with the Newton-Ra Hone standard method in ABAQUS to solve nonlinear problems and to track the nonlinear load-deflection curve of this paper. Newton-Ra's method of the standard non-linear equation is incrementally and repetitively using the matrix of the

Print ISSN: ISSN 2055-6578(Print)
Online ISSN: ISSN 2055-6586(online)

stiffness of the tangent. The modified risk method is generally used to resolve torsion involving an unloading response that uses the load size as an additional unknown and simultaneously unknown displacement. This is achieved using the length of the arc along with the static balance equilibrium in the load-displacement space. Initial increments will be modified if the element model specified in the convergence fails. Finally, the load value is calculated after each increment automatically. The final result will be either the maximum load value or the maximum displacement value.

Finite Element Type and Mesh

After you enter the properties of the material in the multiple parts created for each component, the assembly model is followed. Finally, the next step is assembly meshing.

A well-detailed mesh is a key issue in FEM. The softer the component is, the better the final results. However, the mesh number in the form determines the time of the account required to complete the simulation. A good mesh should contain well-formed elements with mild deformation and moderate side ratios. The meshing profile of all components is illustrated in Figure.19.

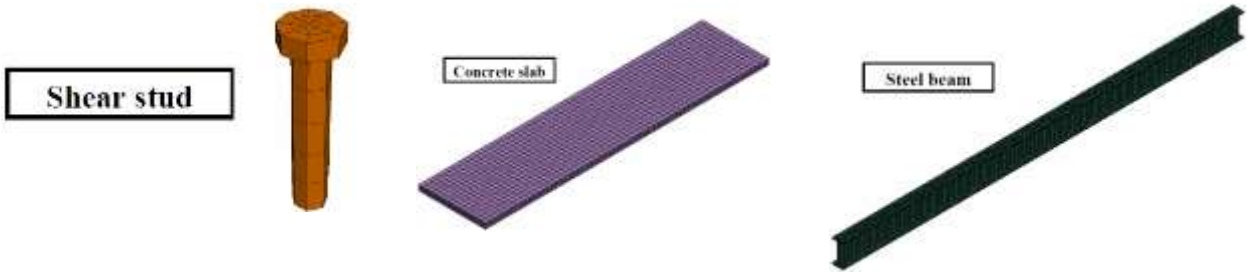

Figure.19 Finite element types and mesh for FEM

Sensitivity Analysis

An analysis of the sensitivity of the finite element modeling of the composite steel-concrete beams in this paper was performed. Since the main failure criterion for composite steel-concrete beams, which is combined flexure and torsion, was either the cracking of the concrete slab because of the torsion or compressive crushing of the concrete slab due to flexure, so the concrete material properties were important in this study.

Also, the mesh size of the concrete slab, steel beam and shear connectors was of great importance, especially in the number of concrete slab layer given to the model. The concrete layer number of the slab can determine the failure in the concrete slab due to torsion, while the size of the mesh for each component can affect the initial behavior of the model regarding stiffness and ultimate final strength as well.

Sensitivity to mesh size

To study the sensitivity of the mesh size of the finite element model of composite steel-concrete beams subjected to flexure and torsion with PSC effects. Different mesh configurations were given to three of

Print ISSN: ISSN 2055-6578(Print)
Online ISSN: ISSN 2055-6586(online)

the main components of metal composite steel-concrete beams that are shear conductors, concrete slabs, and steel beam.

Concrete slab

In Figure.20, the sensitivity of the mesh size of the concrete slab was examined using mesh sizes of 100, 200 and 300 mm. From Figure.21, the results of different sizes of concrete mesh are plotted against the CCBF-1 experimental result. The error percentages were 4, 11 and 14% for the concrete slab's mesh of 100, 200 and 300 mm, respectively. Therefore, the optimum size for the concrete slab was the size of the mesh 100 mm for the finite element model.

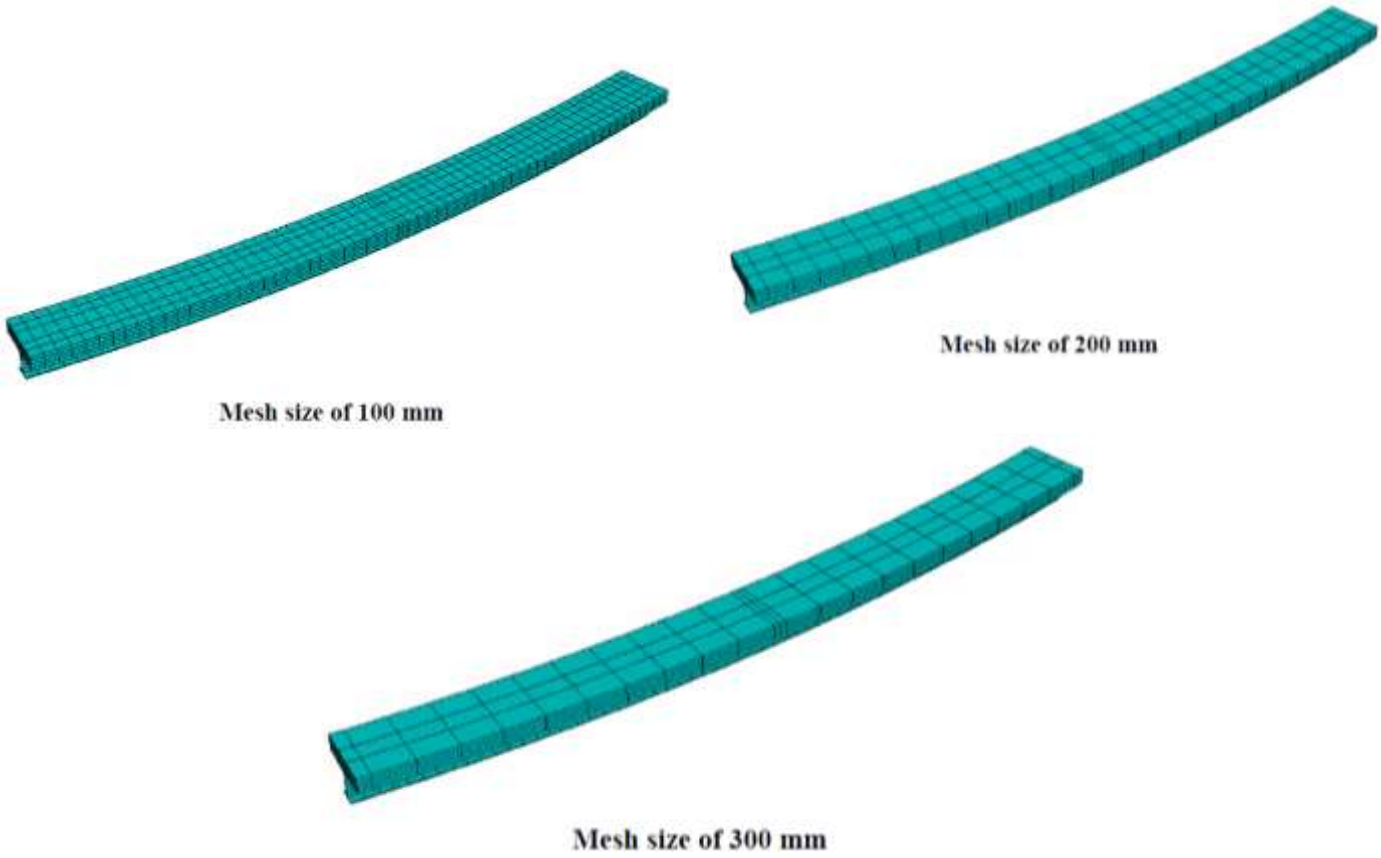

Figure.20 Different mesh sizes for the concrete slab

Print ISSN: ISSN 2055-6578(Print)
Online ISSN: ISSN 2055-6586(online)

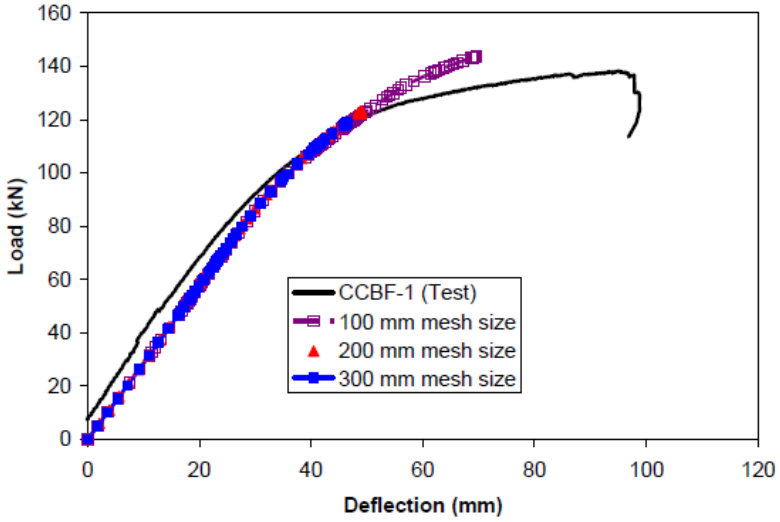

Figure.21 Sensitivity to mesh size for concrete slab

Shear connectors

In Figure.22, four different mesh configurations of shear connectors were provided to investigate the sensitivity of the size of the shear connectors' mesh size to the results of the selected finite element model. The different mesh configurations are based on mesh sizes of 15, 20, 25 and 30 mm for connecting shear meshing.

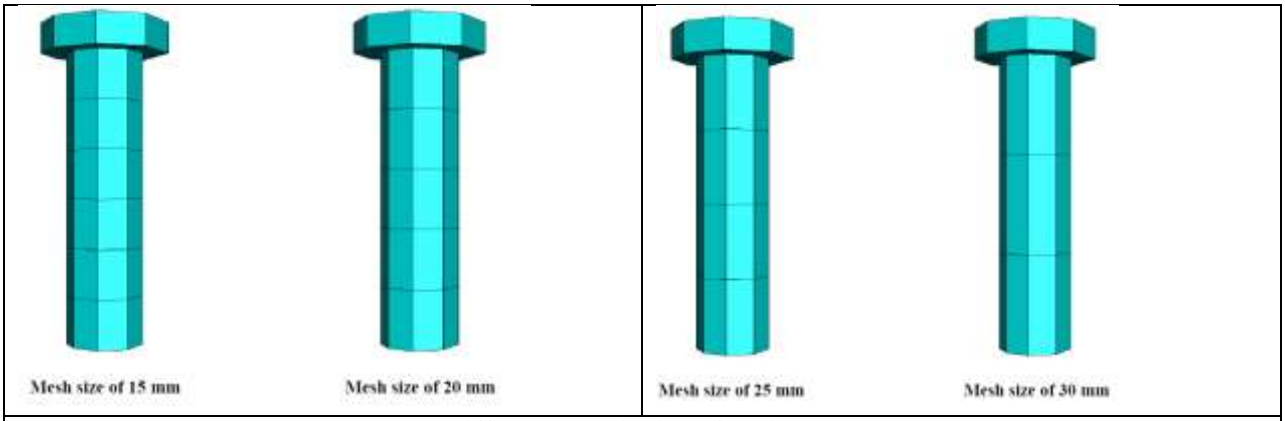

Figure.22 Different mesh sizes for shear connectors

The load deviation curves obtained in Fig.23 are shown for the sensitivity of the mesh to the shear connectors in the selected element model. Results are compared with the experimental result of CBF-1. In Fig. 23, calculated error rates were 3, 1, 1 and 6% for the size of the shear connectors' mesh size of 15, 20, 25 and 30 mm, respectively. The ultimate loading capacity starts at a convergence of 30 mm to 15 mm. However, the optimal mesh size with sufficient accuracy for shear connectors was 20 mm with 1% error for ultimate load capacity.

Print ISSN: ISSN 2055-6578(Print)
Online ISSN: ISSN 2055-6586(online)

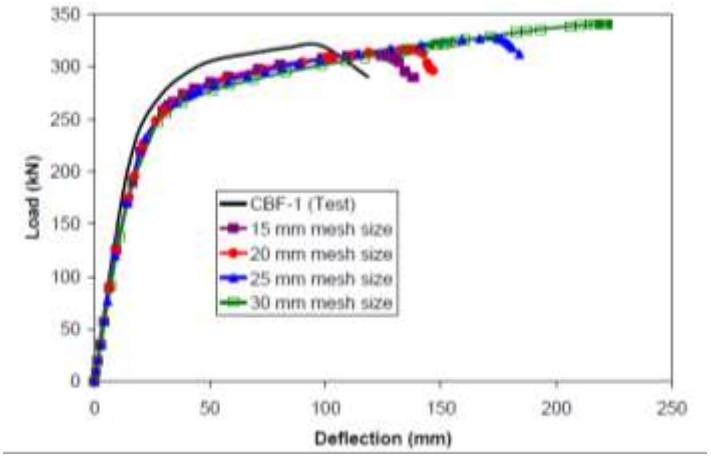

Figure.23 Sensitivity to mesh size for shear connectors

Steel Beam

As for the steel beam, the configurations of the given mesh were 20, 40 and 80 mm mesh sizes as shown in Figure.24.

The load-deflection curves of different mesh configurations are plotted against the CFP-1 experimental result in Fig.25. From the comparison, the percentages of errors 1, 6 and 20% of the mesh size of the steel beam were 20, 40 and 80 mm respectively. As shown in Figure 6.16, the mesh size of 40 and 80 mm was not sufficient to predict CBP-1 behavior regarding ductility and load capacity. Therefore, a 20 mm mesh size for the steel beam was used in the selected finite element model.

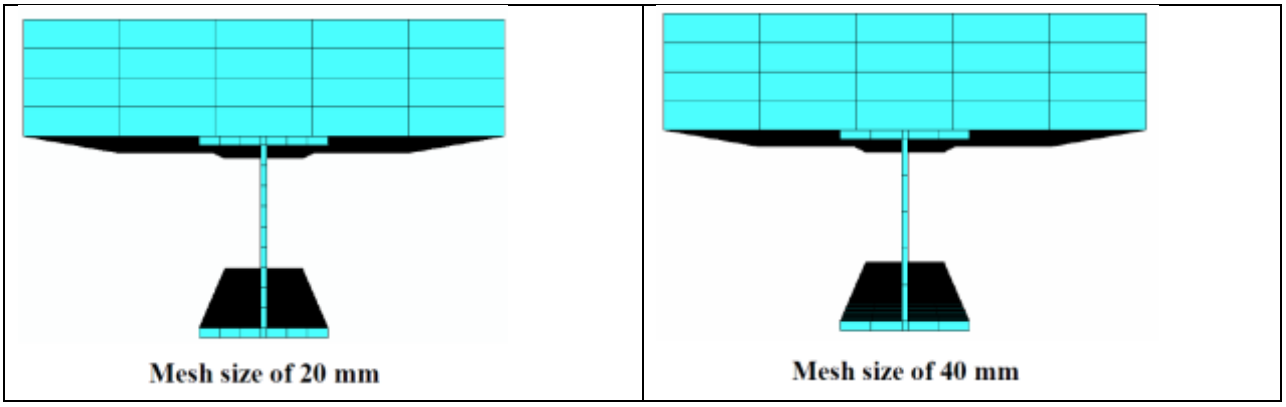

Print ISSN: ISSN 2055-6578(Print)
Online ISSN: ISSN 2055-6586(online)

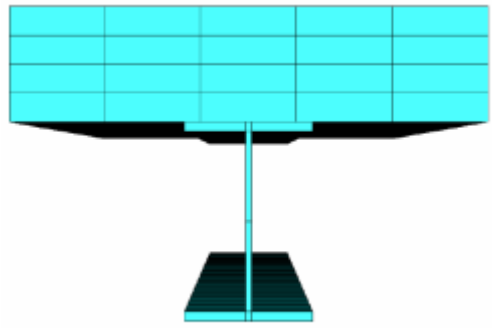

Mesh size of 80 mm

Figure.24 Different mesh sizes for steel beam

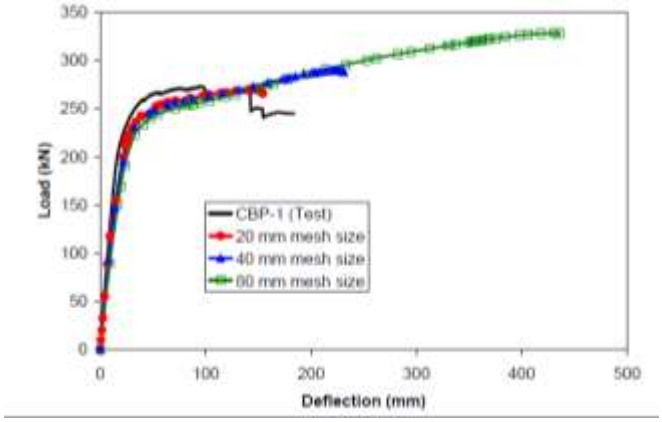

Figure.25 Sensitivity to mesh size for steel beam

RESULT AND DISCUSSION

The accuracy of the finite element model was validated by comparing the experimental results of the composite steel-concrete beams subjected to combined flexure and torsion combined with PSC effects. The experimental series was carried out to examine the behavior of straight composite steel-concrete beams, six concrete slabs where flexure and torsion. The full details of the test specimens are combined with their corresponding material properties in their respective chapters. Comparisons were made between each test specimen in each model. FEM reliability was created by comparing experimental results with model results regarding load-deflection response and ultimate strength capabilities.

Comparisons between Models and Experimental

To validate FEM, comparisons were made with the experimental results of straight six straight composite steel-concrete beams (CBF1 to CBF-3 and CBP-1 to CBP-3). Beam details including

Print ISSN: ISSN 2055-6578(Print)
Online ISSN: ISSN 2055-6586(online)

material properties of the components obtained from the relevant material tests are shown in Tables.6.

Table.6 Composite beam details for experimental

	Reference	Chapter 3
	Beam identification	CBF-1, CBF-2, CBF-3,
		CBP-1, CBP-2, CBP-3
	Span length (mm)	4100
Concrete slab	Thickness (mm)	120
	Width (mm)	500
	Compressive strength (N/mm^2)	26.7
	Tensile strength (N/mm^2)	3.23
Steel beam	Type	200UB29.8
	Gross area (mm^2)	3820
	Total depth (mm)	207
Steel flange	Thickness (mm)	9.6
	Yield stress (N/mm^2)	341
	Ultimate stress (N/mm^2)	495
Steel web	Thickness (mm)	6.3
	Yield stress (N/mm^2)	355
	Ultimate stress (N/mm^2)	510

The results of the beams are compared regarding the mid-term load-deflection response. Each comparison was discussed in Section 4.1.1.

Validation of the finite element model

Composite steel-concrete beam

Composite steel and concrete beam designed with FSC and only a pure flexure in the experimental. The details of properties described above as table.6

From Figure.26 below, the load-deflection curve of the model has a good agreement with the experimental results of specimens. The curve provides a similar peak load and shows a similar ductility to specimens. The model also indicated a decrease in load applied due to the failure of the shear connectors similar to experimental specimens.

Print ISSN: ISSN 2055-6578(Print)
Online ISSN: ISSN 2055-6586(online)

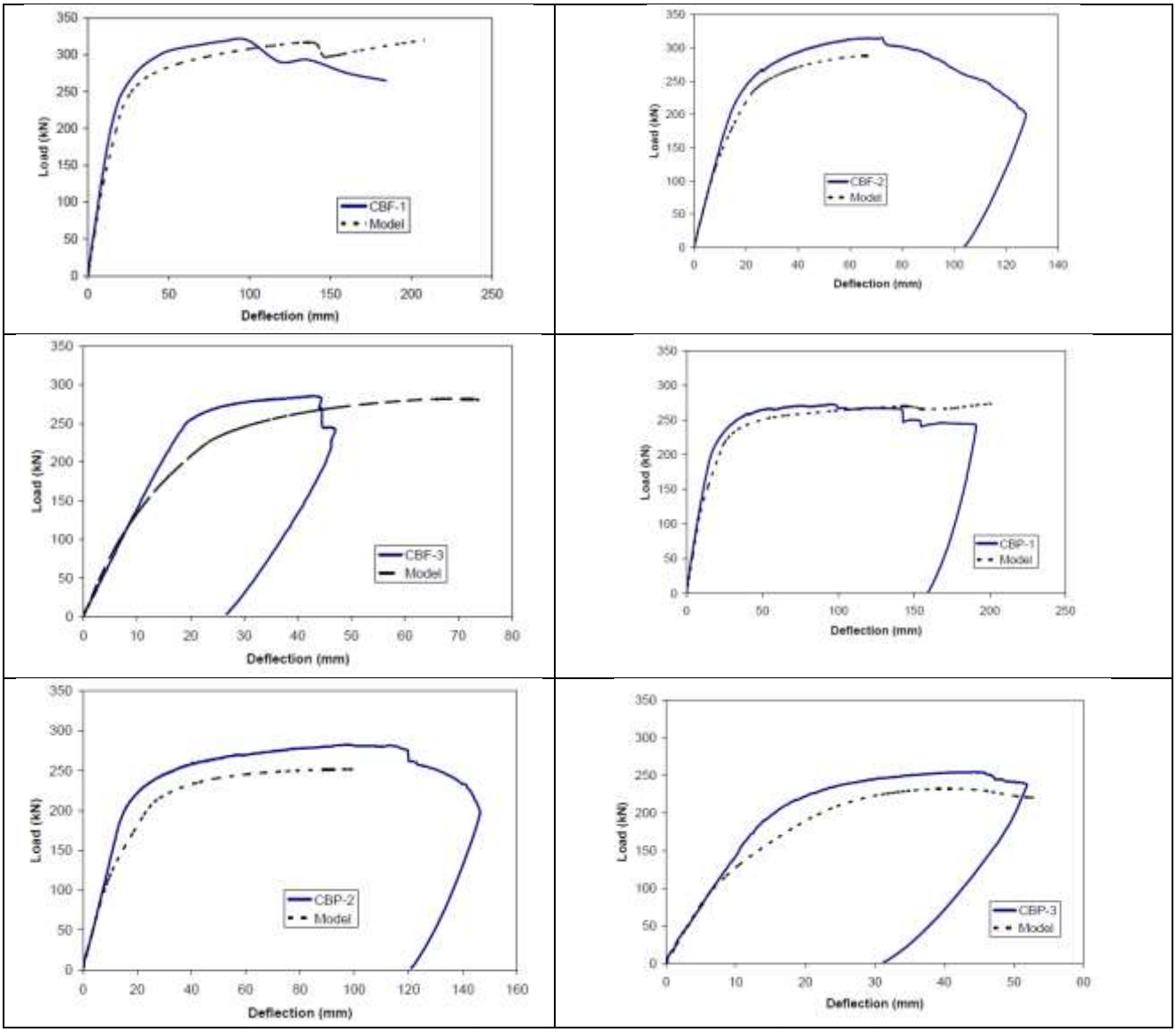

Figure.26 Comparisons between FEM and Experiment

4.1.1.1 Comparisons of the finite element model

From Figs.27 and 28, FEM cross-sectional are displayed at the loading point for CBF and CBP, respectively.

Print ISSN: ISSN 2055-6578(Print)
Online ISSN: ISSN 2055-6586(online)

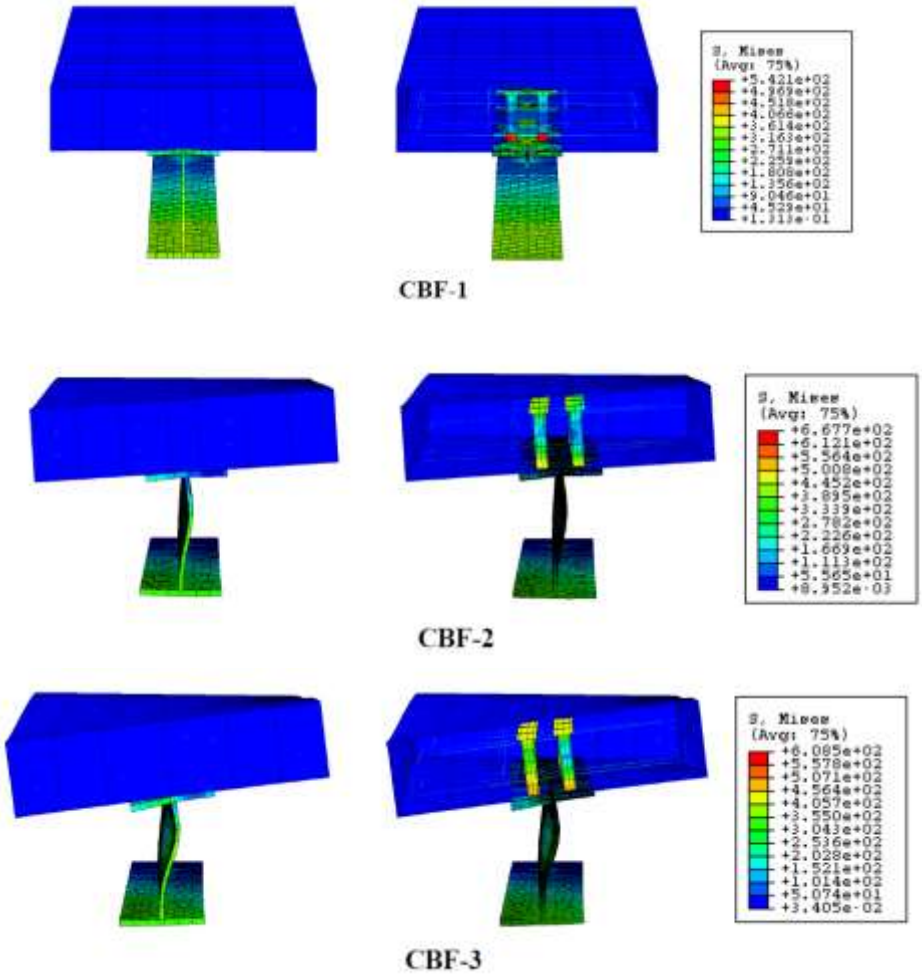

Figure.27 Cross-sectional views of FEM at point load for CBF

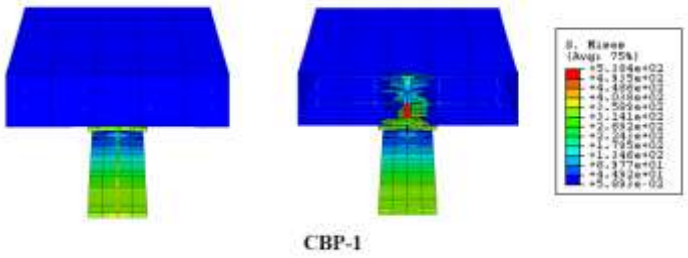

Print ISSN: ISSN 2055-6578(Print)
Online ISSN: ISSN 2055-6586(online)

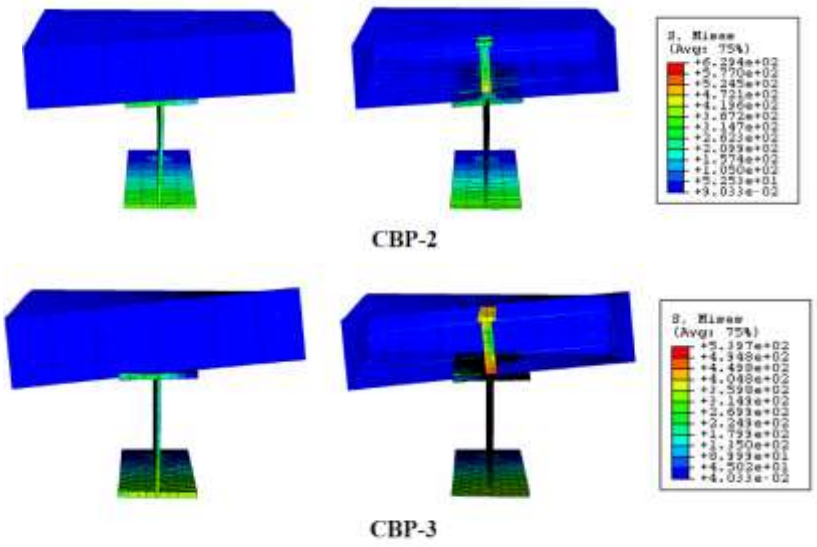

Figure.28 Cross-sectional views of FEM at point load for CBP

It can be observed that the stress regions of the shear connectors were greatest when the composite steel-concrete beams were subjected to pure flexure, for example, CBF-1 and CBP-1. However, the stress regions for the shear connectors on CBF-3 and CBP-3 were greater than CBF-2 and CBP-2 due to excessive torsion of the concrete slab especially in the main regions of shear connectors.

Also, the twisted angles of the concrete slabs were different from the steel beams as shown in Figs.27 and 28 for composite steel-concrete beams exposed to flexure and torsion such as CBF-2, CBF-3, CBP-2, and CBP-3. This observation supported the conclusion that the curvature of the concrete slab and the steel beam were different in a composite steel-concrete beam that underwent flexure and torsion during the test.

This indicates the flexible concrete cracking of CBF-1 and CBP-1, whereas it is a combination of the torsional and flexural concrete cracking of CBF-2, CBF-3, CBP-2, and CBP-3.

Discussion

There was generally good agreement between experimental results and finite element models in terms of the relationship of load-deflection during the entire loading profile until failure. The initial stiffness, ultimate flexural and torsional moment capacities are closely designed. For beams governed by torsional failure, it can be observed that the analysis was able to predict this with reasonable accuracy. Even for beams under the pure flexure, the ductility or other post failure showed in the models for CBF-1, CBP-1.

Based on the accuracy of the results from the experimental-numerical comparisons, it can be concluded that the numerical model of ABAQUS in above is appropriate and reliable to simulate the

Print ISSN: ISSN 2055-6578(Print)
Online ISSN: ISSN 2055-6586(online)

behavior of straight composite steel-concrete beams. The relationship between load deflections of modeling was accurately managed. For beams exposed to combined flexure and torsion, the failure mode was not subject to fracture the connector. This was also reasonably predicted from the model. In Table.7, provides a summary of the digital comparison between experimental and analytical results regarding flexural and torsional moment capabilities.

Table 6.7 Comparison table regarding ultimate strengths

Beam	***B*** (%)	Ultimate flexural moment (KN.m)			Ultimate torsional moment (KN.m)		
		Test	FEM	Ratio (FEM / Test)	Test	FEM	Ratio (FEM / Test)
CBF-1	100	220	218	0.99	N/A	N/A	N/A
CBF-2	100	214	198	0.93	17	15	0.88
CBF-3	100	197	193	0.98	28	25	0.89
CBP-1	50	188	186	0.99	N/A	N/A	N/A
CBP-2	50	194	193	0.99	16	14	0.88
CBP-3	50	177	159	0.90	24	20	0.83
Avg.		0.98			0.97		
Std. Dev.		0.11			0.15		

The comparison was accurate with the model to test the result ratios close to one. The initial stiffness of the model was considered satisfactory in the view of a non-linear rise in the behavior of composite steel-concrete beams.

Partial strength behavior was shown in the model with the difference in the ultimate flexural strength of CBF-1 and CBP1 composite steel-concrete beams. A longitudinal interface slip of the model was observed for both the FSC and PSC steel composite steel-concrete beams.

Print ISSN: ISSN 2055-6578(Print)
Online ISSN: ISSN 2055-6586(online)

CONCLUSION

The main objective of this paper was to study the effects of PSC on the behavior of composite steel-concrete beams subjected to combined flexure and torsion.
These six components were implemented through a paper.
Most importantly, this model was used to monitor the standard of failure due to torsion.
The comparison between FEM and the experimental results was confirmed by the 3-D FEM in terms of the response of the load-deflection and the ultimate strengths. Using the verified model, a parametric study was performed in above with parameters such as the different length of the span and different shear connection levels. All these works have implemented all six objectives of this paper with detailed and comprehensive implementation.

Acknowledgment

The research reported in the paper is part of the Project 71256481 supported by IBB University, at the end of this work, I am grateful to many people who helped me to finish this paper: for my entire classmate.

Author Contributions:
All authors contributed to conceiving the paper, analysis the date, mapping and Plotting.

Conflicts of Interest:
The authors declare no conflict of interest.

REFERENCES

[1] American Institute of Steel Construction (2006) *AISC steel constructional manual*, American Institute of Steel Construction.
[2] Baskar, K. and Shanmugam, N.E. (2003) "Steel-concrete composite plate girders subject to combined shear and bending", *Journal of Constructional Steel Research*, 59, 531-557.
[3] Baskar, K., Shanmugam, N.E. and Thevendran, V. (2002) "Finite-element analysis of steel-concrete composite plate girder", *Journal of Structural Engineering*, ASCE, 128(9), 1158-1168.
[4] British Standards Institution (2004) *BS5950-1, Structural use of steelwork in* a *building, Part 1: Code of practice for design-rolled and welded sections*, British Standards Institution, London.
[5] British Standards Institution (2005) *Eurocode 4: Design of composite steel and composite structures, Part 1.1 General rules and rules for buildings, DDENV 1994-1-1*, European Committee for Standardisation (CEN).
[6] Carlsson, M.L.R. and Hajjar, J.F. (2000) "Fatigue of stud shear connectors in the negative moment region of steel girder bridges: a synopsis of experimental results and design

Print ISSN: ISSN 2055-6578(Print)
Online ISSN: ISSN 2055-6586(online)

recommendations", *Final Report*, The Center for Transportation Studies, University of Minnesota.

[7] Fabbrocino, G., Manfredi, G. and Cosenza, E. (2000) "Analysis of continuous composite beams including partial interaction on bond", *Journal of Structural Engineering*, ASCE, 126(11), 1288-1294.

[8] Karlsson, B.I. and Sorensen, E.P. (2006a) *ABAQUS: Analysis user's manual version 6.5*, Pawtucket, Rhode Island, Hibbitt Publication.

[9] Karlsson, B.I. and Sorensen, E.P. (2006b) *ABAQUS: Analysis user's manual volume IV: Element*, Pawtucket, Rhode Island, Hibbitt Publication.

[10] Karlsson, B.I. and Sorensen, E.P. (2006c) *ABAQUS: Analysis user's manual volume V Prescribed conditions, constraints and interactions*, Pawtucket, Rhode Island, Hibbitt Publication.

[11] Lam, D. and El-Lobody, E. (2005) "Behavior of headed stud shear connectors in composite beams", *Journal of Structural Engineering*, ASCE, 131(1), 96-107.

[12] Liang, Q.Q., Uy, B., Bradford, M.A. and Ronagh, H.R. (2004) "Ultimate strength of continuous composite beams in combined bending and shear", *Journal of Constructional Steel Research*, 60(8), 1109-1128.

[13] Liang, Q.Q., Uy, B., Bradford, M.A. and Ronagh, H.R. (2005) "Strength analysis of steel-concrete composite beams in combined bending and shear", *Journal of Structural Engineering*, ASCE, 131(10), 1593-1600.

[14] Loh, H.Y., Uy, B. and Bradford, M.A. (2004a) "The effects of partial shear connection in the hogging moment regions of composite beams Part I – Experimental study", *Journal of Constructional Steel Research*, 60, 897-919.

[15] Loh, H.Y., Uy, B. and Bradford, M.A. (2004b) "The effects of partial shear connection in the hogging moment regions of composite beams Part II – Analytical study", *Journal of Constructional Steel Research*, 60, 921-962.

[16] Mirza, O. and Uy, B. (2009a) "Effects of steel fibre reinforcement on the behaviour of headed stud shear connectors for composite steel-concrete beams", *Advanced Steel Construction*, 5(1), 72-95.

[17] Mirza, O. and Uy, B. (2009b) "Behaviour of headed stud shear connectors for composite steel-concrete beams at elevated temperatures", *Journal of Constructional Steel Research*, 65, 662-674.

[18] Nie, J., Luo, L. and Hu, S. (2000) "Experimental study on composite steel-concrete beams under combined bending and torsion", *Composite and Hybrid Structures*, 2, 631-638.

[19] Nie, J., Tang, L. and Cai, C.C. (2009) "Performance of steel-concrete composite beams under combined bending and torsion", *Journal of Structural Engineering*, ASCE, 135(9), 1048-1057.

[20] Pi, Y.L., Bradford, M.A. and Uy, B. (2006) "Second order nonlinear analysis of steel-concrete members. II: Applications. *Journal of Structural Engineering*, ASCE, 132(5), 762-771.

Print ISSN: ISSN 2055-6578(Print)
Online ISSN: ISSN 2055-6586(online)

[21] Rex, C.O. and Easterling, W.S. (2002) "Partially restrained composite beam-girder connections", *Journal of Constructional Research*, 58, 1033-1060. Scott, W.B.

[22] Sebastian, W. and McConnel, R.E. (2000) "Nonlinear finite element analysis of steel-concrete composite structures", *Journal of Structural Engineering*, ASCE, 126(6), 662-674.

[23] Standards Australia (2000) *Australian Standard AS 1012.10-2000, Methods of testing concrete – determination of the indirect tensile strength of concrete specimens (Brasil or splitting test)*, Standards Australia International Ltd.

[24] Standards Australia (2002) *Australian/New Zealand Standard AS/NZS1170.1-2002, Structural design actions Part 1: Permanent, imposed and other actions* Standards Australia International Ltd.

[25] Standards Australia (2003) *Australian Standard AS2327.1-2003, Composite structures Part 1: Simply supported beam*, Standards Australia International Ltd.

[26] Tan, E.L. and Uy, B. (2005) "Effects of partial shear connection on the strength and ductility of semi-continuous composite beams", *Developments in Mechanics of Structures & Materials*, 181-187.

[27] Thevendran, V., Chen, S., Shanmugam, N.E. and Richard Liew, J.Y. (2000) "Experimental study on steel-concrete composite beams curved in a plan", *Engineering Structures*, 22, 877-889.

[28] Uy, B. and Liew, J.Y. (2003) *The civil engineering handbook*, CRC Press, USA.

Print ISSN: ISSN 2055-6578(Print)
Online ISSN: ISSN 2055-6586(online)